EVALUATION OF THE ILLUMINATION GEOMETRY EFFECTS ON THE TARGET SURFACE REFLECTANCE ESTIMATED FROM AVIRIS DATA

LUIZ ALBERTO VIEIRA DIAS[1]
MARCELO LOPES LATORRE[2]
EDUARDO JORGE DE BRITO BASTOS[1]

1.   UNIVAP – Paraíba Valley University - IP&D – Institute for Research and Development
Avenue Shishima Hifumi, 2911- 12244-000 São José dos Campos, SP, Brasil
vdias@univap.br

2.   CTA – Aerospace Technological Center-IEAv – Institute for Advanced Studies
12228-580 São José dos Campos, SP, Brazil
latorre@ieav.cta.br

1 Introduction

Remote sensing is based on the identification and discrimination among targets, in which the radiance detected by a sensor, is the basis of this process. This mechanism of acquisition of data would be the ideal if the spectral and temporal of information contents always stayed unaffected. However, this doesn't happen, since between the sensor and the surface there is an extremely dynamic medium, the atmosphere, that interacts with the electromagnetic radiation. Such interaction provokes alterations in the propagation of the radiation flow from the target. As a consequence of that interaction process, the distribution of the surface radiance of the observed radiance by a sensor is different from the intrinsic radiance emitted by the surface. The net effect is that the data obtained through remote sensing are just apparent, which affects directly the applications of remote sensing to the Meteorology and the Natural Resources.

The spectral reflectance is an element of the spectral behavior of each surface feature. The factors that influence the determination of the reflectance and, consequently, the spectral characteristics, are: the data acquisition geometry, the relative parameters of the target, and the atmospheric parameters such as humidity, concentration and type of aerosols, cloud cover, etc. (Bokwer et al., 1985).

In this way, the importance of knowing the atmospheric optical properties, and how electromagnetic radiation interacts with its constituents becomes apparent, especially when creating or using the several necessary methods of atmospheric correction to minimize atmospheric effects.

Thus, the general objective of this work is to apply a method of atmospheric correction that emphasizes the strong influence of the effects of the illumination geometry in its final results and shows the importance of trying to minimize these effects. Spectra of green vegetation targets (riparian forest), of exposed soil, and of bodies of water, extracted directly from the images, are used as reference for the discussions studied in this work. Of the several existing methods used for atmospheric correction the method developed by Green et al. (1993) for the atmospheric correction of hyperspectral images was chosen. Data for this study were obtained from an AVIRIS (Airborne Visible/Infrared Imaging Spectrometer) sensor (Latorre, 1998).

2 - Study Area

The AVIRIS sensor was used during the experiment SCAR-B accomplished in Brazil from August to September 1995; our objective was the study of particles in suspension in the air (aerosols). In this mission three aircraft were involved: a) Earth Resources ER-2 of the AMES Research Center of NASA, b) Convair C-131A from the University of Washington, and c) Bandeirante EMB-110 of INPE (SCAR-B, 1996).

During this experiment we obtained images by the AVIRIS sensor (equipped in the aircraft ER-2) of the following regions: Brasília (DF), Cuiabá (MT), Swampland of Mato Grosso (MS), Porto Nacional (GO), Alta Floresta (MT), Vilhena and Ji-Paraná (RO).

In this work we used images of the Cuiabá area (Figure 1). The reason for this choice, is due to the fact that this is the only region in which it was possible to obtain images under three different atmospheric conditions, in three different days, facilitating in this way the verification of the effects of the acquisition geometry into the employed correction process.

The area of Cuiabá is located in the State of Mato Grosso, Brazil and there prevails the rainy tropical climate (hot and humid). This area is characterized by two different seasons: a dry one, and a rainy one. The first usually embraces a longer period, although it presents some days of rain. The lapse of May to September corresponds to the time of the year in which there is drought. The mean temperature of the area is around 25°C (RADAMBRASIL, 1982). Some of the soil types of larger predominance in the area are of the following classes: Yellow Latossolo, Latossolo red-darkness, Latossolo roxo, Cambissolo and Alluvial Soils. The vegetation cover is characterized by five domains: Savannah, Dense Forest (Ombrófila), Open Forest (Ombrófila) (RADAMBRASIL, 1982).

Fig.1 – Scene common to the three images used in this study around Cuiabá, MT, Brazil, with the three selected targets indicated inside of the squares: yellow (vegetation), cyan (water) and green (soil).

The Figure 1 represents the common area to the three images and the objectives selected for the study. These targets: vegetation, water and bare soil, are represented by samples of 26 pixels identified inside of the squares: yellow (clear gray sample), cyan (green sample), and green (dark gray sample), respectively.

3 - Method of Atmospheric Correction

The method developed by Green et alia (1993) it based on the Radiative Transfer Theory. It was developed for atmospheric correction of hyperspectral images, obtained from the AVIRIS sensor. This method is based on the MODTRAN 3 model, on the calibration of the AVIRIS sensor for the obtained radiance in laboratory, and on calibration from inflight data. The referring calibration data to the year of 1995, were obtained in Ivanpah Playa's area, California (Crósta, 1997).

In this correction type some conditions are pre-established:
1. multi-scattering terrain aspects are not considered;
2. accentuated topographical variations are not considered;
3. the atmospheric albedo should be neglected for high visibility conditions;
4. it is supposed that the terrestrial surfaces targets are Lambertian;
5. the atmosphere is defined as homogeneous horizontally stratified.

The objective of this method is to calculate the reflectance at the terrain surface, from the data of total radiance measured by AVIRIS. For this method, the reflectance value is calculated as a function of the total radiance, of the solar irradiance on the atmospheric top, on the reflectance of the atmosphere and on the atmospheric transmittance in two ways (from the sensor to the surface and from the surface to the sensor), on the path traveled by the electromagnetic energy. More information about the method can be obtained by Green et alia (1993).

4 - Methodology

This methodology comprises the following steps. In order to verify the behavior of the employed method in the correction of identical targets, obtained under different atmospheric and illumination geometry conditions, comparisons were accomplished among the corrected spectra of the mentioned targets of the Cuiabá images for the days 08/25/1995 and 08/27/1995 (with wide differences in the illumination geometry); and for the days 08/25/1995 and 09/07/1995 (with close illumination geometry). These relative comparisons were made in the estimate of the normalized mean square error normalized between two spectra of each selected targets obtained by the following equation (Pitas and Venetsanopaulos, 1990):

$$emq = \frac{\sum_{i=1}^{224}(\rho cor_i - \rho ncor_i)^2}{\sum_{i=1}^{224}(\rho cor_i)^2} *100$$

where,

ρcor_i = Value of the surface reflectance (corrected)of the band i;
$\rho ncor_i$ = Value of the apparent reflectance (non corrected) of the band i.

For these calculations an algorithm was developed, which is capable to determine the two mentioned spectra, showing its differences in normalized square medium errors (%). All these procedures were accomplished for the three targets (Latorre, 1998).

5. Results and Discussions

In these analyses the comparisons were made between the images of 08/25 and 08/27 and also between the images of 08/25 and 09/07, in this sequence, using the targets: vegetation, water, and bare soil. Table 1 indicates the different values of azimuth and elevation angles for the selected images.

TABLE 1 - AZIMUTH AND ELEVATION ANGLES FOR THE SELECTED IMAGES

	Image 08/25	Image 08/27	Image 09/07
Azimuth angle	4.3°	58.9°	9.5°
Elevation angle	64°	45°	67°

The first analysis was accomplished with the spectrum of the riparian forest sample on 08/25 and the sample 08/27 (Fig.2); and for the sample 08/25 and the sample 09/07 (Fig.3). These were followed by the analyses of the spectra of the samples of water (Fig.4 and 5) and bare soil (Fig.6 and 7), respectively. These figures present the analyses in the range of 0.4μm to 2.5μm, with its respective normalized square mean errors for the considered range.

Observing Figure 2, it is noticed that the spectra are very similar. In the area of the visible, the spectra present a difference (2.88%) that can be explained possibly by the non consideration of the effects of surface anisotropy, as well as by the fact that the method does not correct in a satisfactory way the effects of the atmospheric scattering for atmospheres saturated by aerosols. In this range the backscatter effects should also be considered. The smaller the elevation angle, the larger the backscatter, caused mainly by the increase of the shadow on the vegetation. In the infrared range, the observed difference may possibly be explained by the different elevation and azimuth angles, and in smaller proportions, by shadow effects, and wind, among others.

It is still observed in the infrared range that the elevation angle (illumination geometry) influences the reflectance of the vegetation. Since the image of 08/25 has an elevation angle (64°) larger than the one of the image of the 08/27 (45°), it is verified, in Figure 2, that the reflectance values are higher.

In this range, where the atmospheric influence (scattering) is smaller, the reflectance values of 08/25 are larger than the ones of 08/27, showing that, the larger the elevation angle, the smaller the shadow effect, and larger the target reflectance. This difference will be smaller if the elevation angles are close to each other, as it can be observed in the Figure 3 (1.83%).

Considering in this case, that the differences of the elevation angles are very small, Figure 3 shows almost an overlap of the spectra in the range of the near infrared. However, the difference continues in the visible range of the spectrum, explained possibly by the fact that the method does not correct in a satisfactory way the scattering effect, on aerosol saturated environments, keeping the difference between them.

The differences verified for the vegetation spectra are also observed when comparing the spectra corrected for the atmospheric effects for bare soil and water. In Figure 4 (water) and in Figure 6 (bare soil), where the images were acquired with different elevation angles (different illumination geometry), it is observed that the differences among the spectra are of 24.77% and 2.19%, respectively. However, it can be observed that these differences are reduced for images with similar values of elevation angle (12.68%) for the case of the water in Figure 5, and 0.35% for the soil in Figure 7. This shows again the strong influence of the illumination geometry effects on the analysis of these targets.
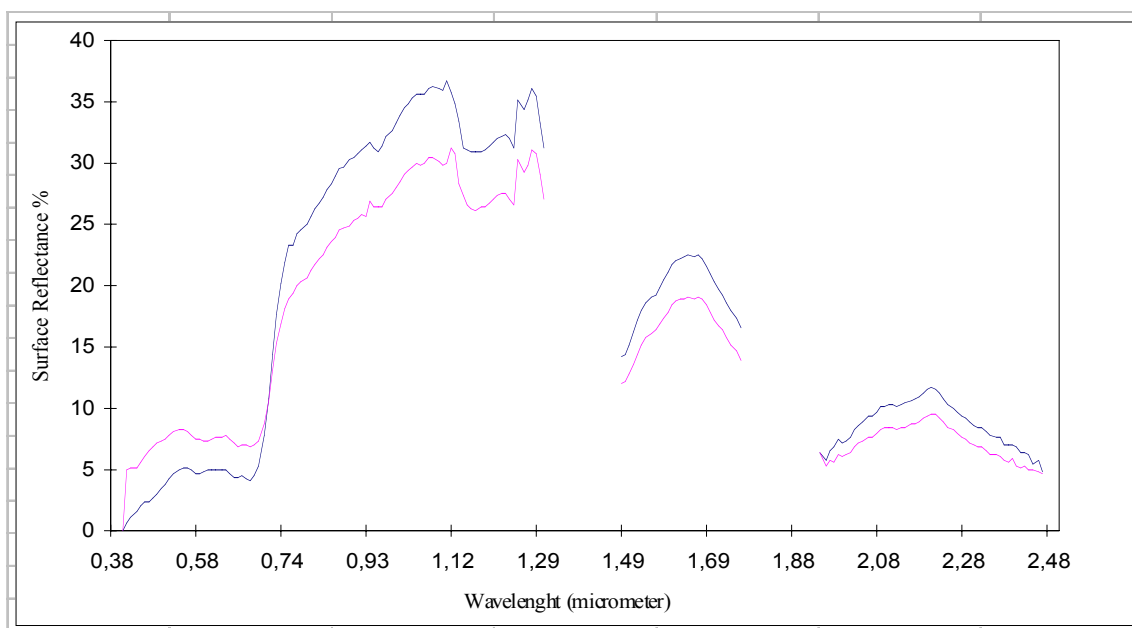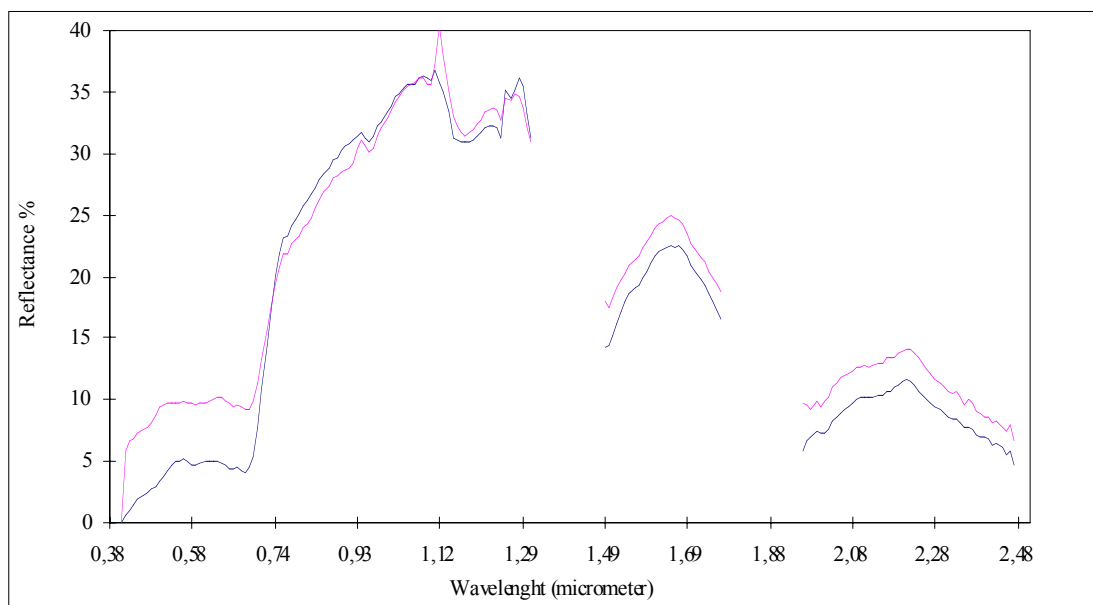
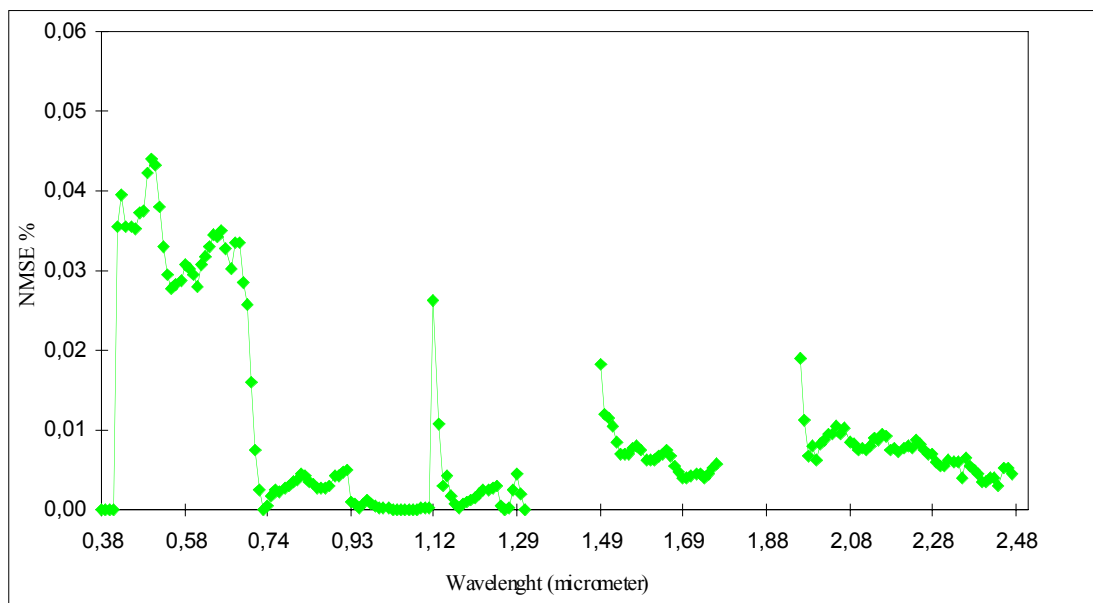Normalized mean square error between the two reflectance spectra (below)
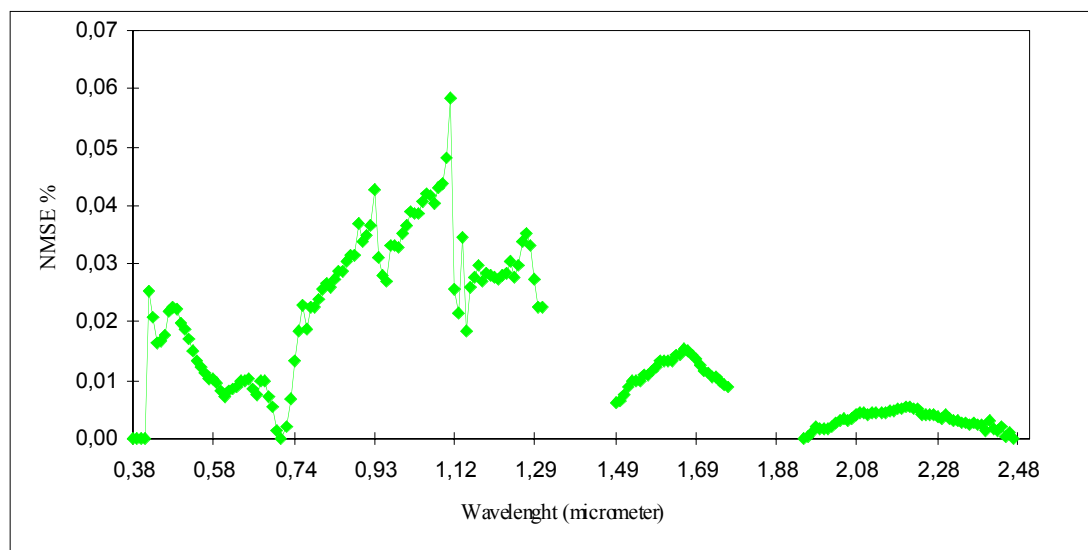
Normalized Square Mean Error (%) on range (0,38-2,5μm)	2.88

Fig.2 - Difference between the spectra corrected for atmospheric effects of a sample of riparian vegetation (08/25/1995 and 08/27/1995), in the spectral range from 0.38mm to 2.5mm, with its respective normalized mean square errors.
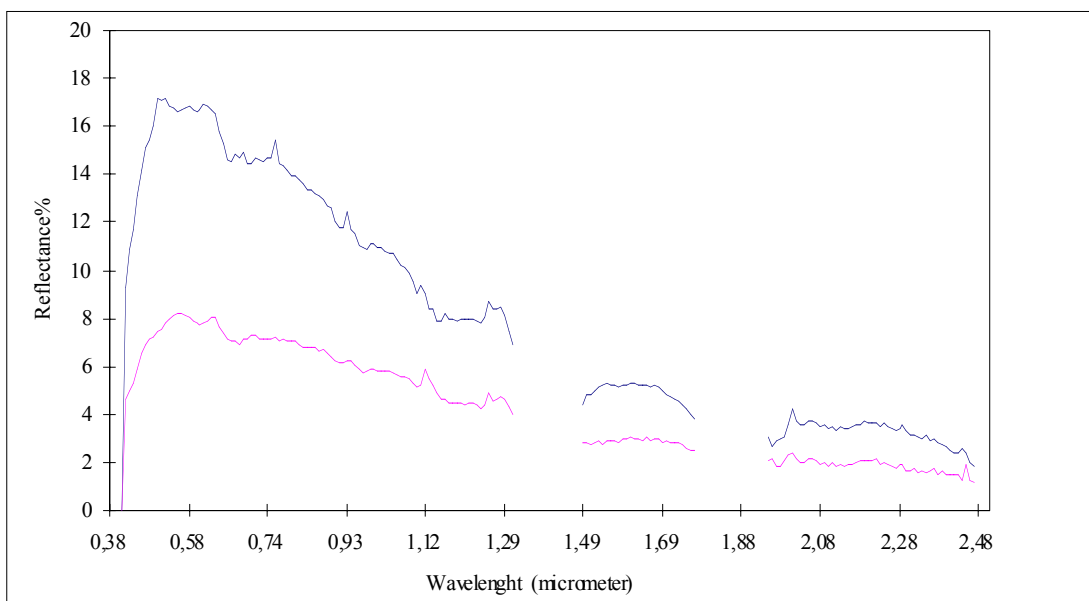
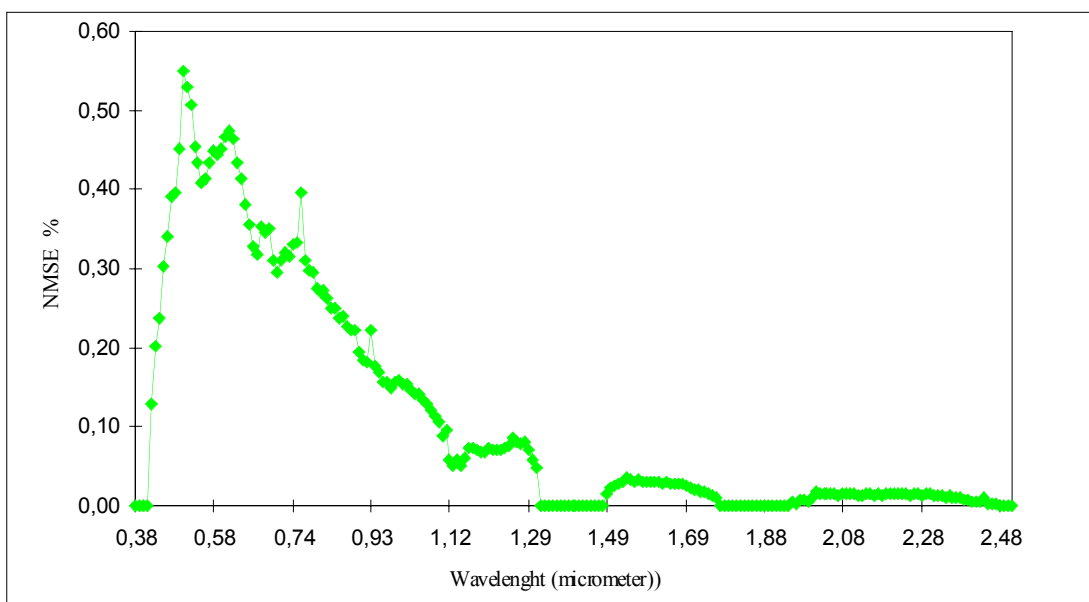Normalized mean square error between the two reflectance spectra (below)

Normalized Square Mean Error (%) on range (0,38-2,5µm)	1.83

Fig.3 - Difference between the spectra corrected for atmospheric effects of a sample of riparian forest (08/25/1995 and 09/07/1995), in the spectral range from 0.38µm to 2.5µm, with its respective normalized mean square errors.
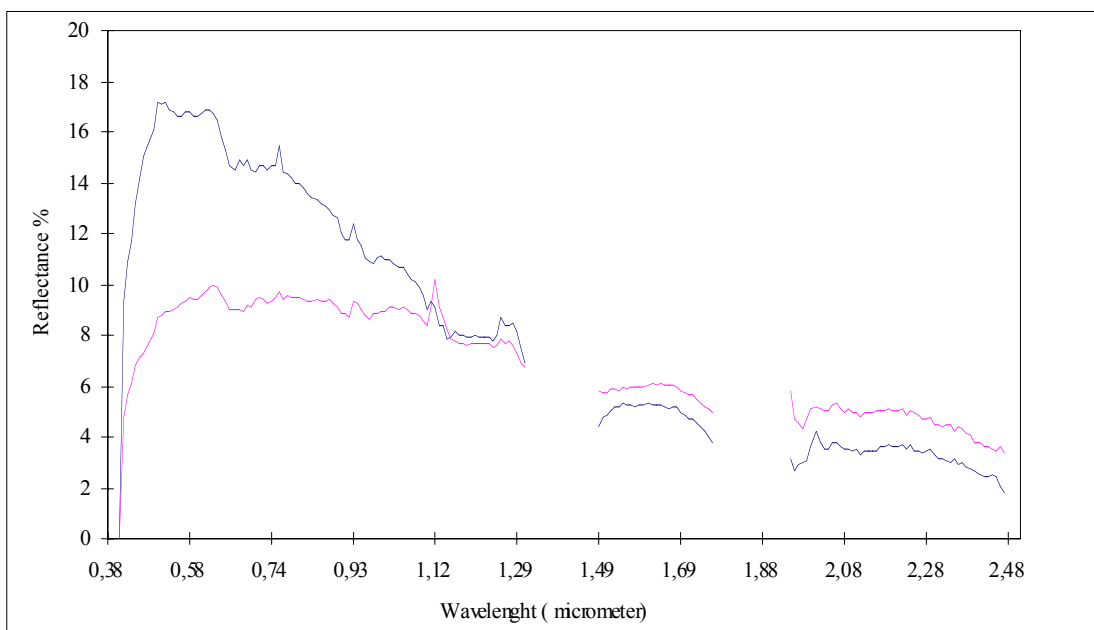
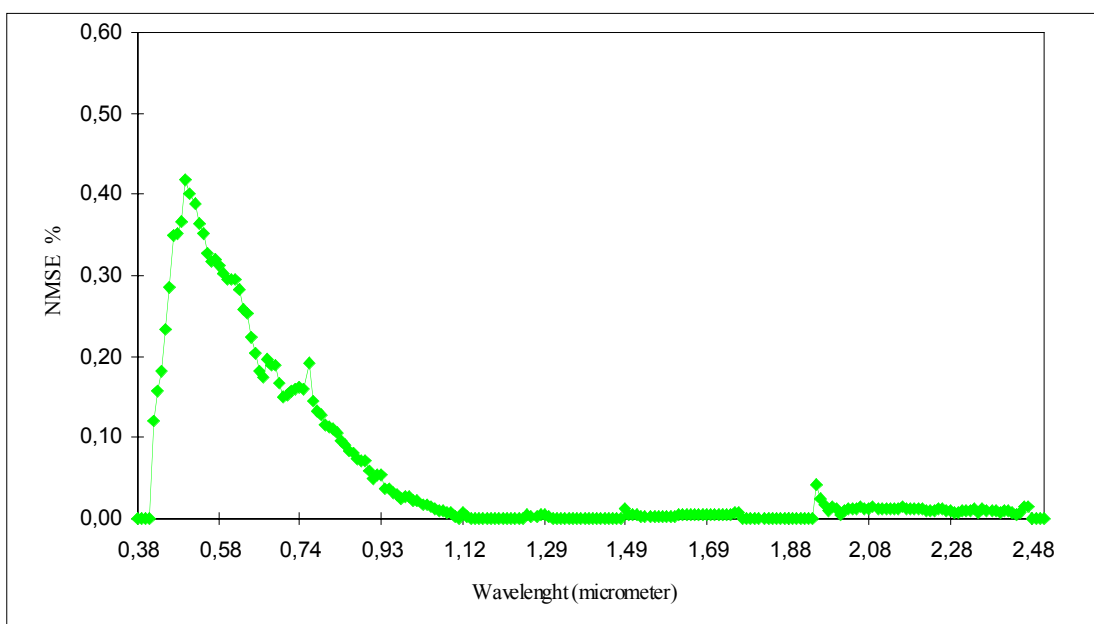Normalized mean square error between the two reflectance spectra (below)

Normalized Square Mean Error (%) on range (0,38-2,5µm)	24.77

Fig.4 - Difference between the spectra corrected for atmospheric effects of a sample of body of water (08/25/1995 and 08/27/1995), in the spectral range from 0.38µm to 2.5µm, with its respective normalized mean square errors.
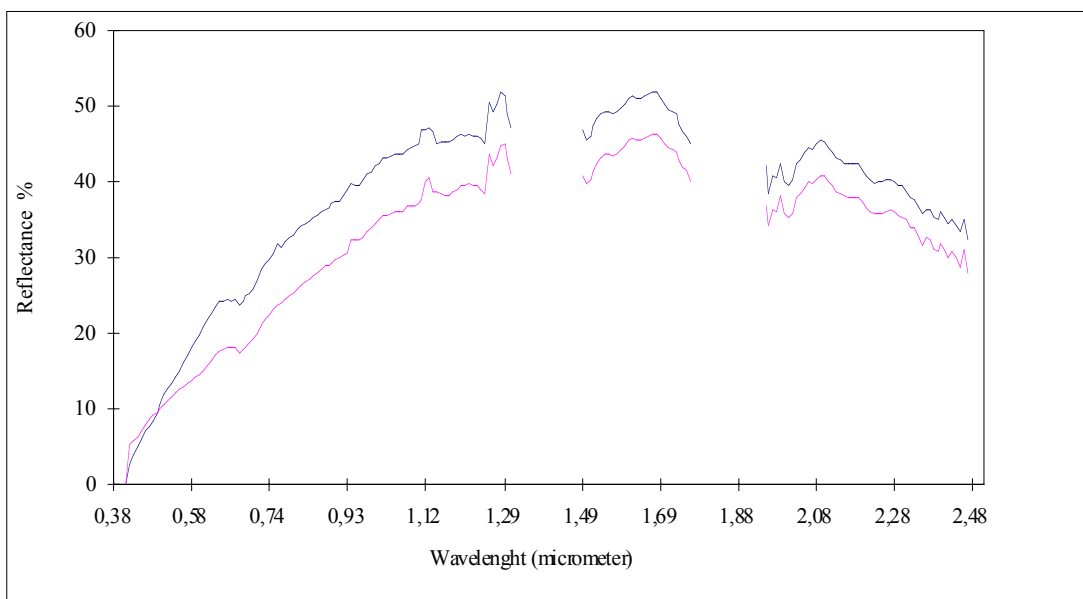
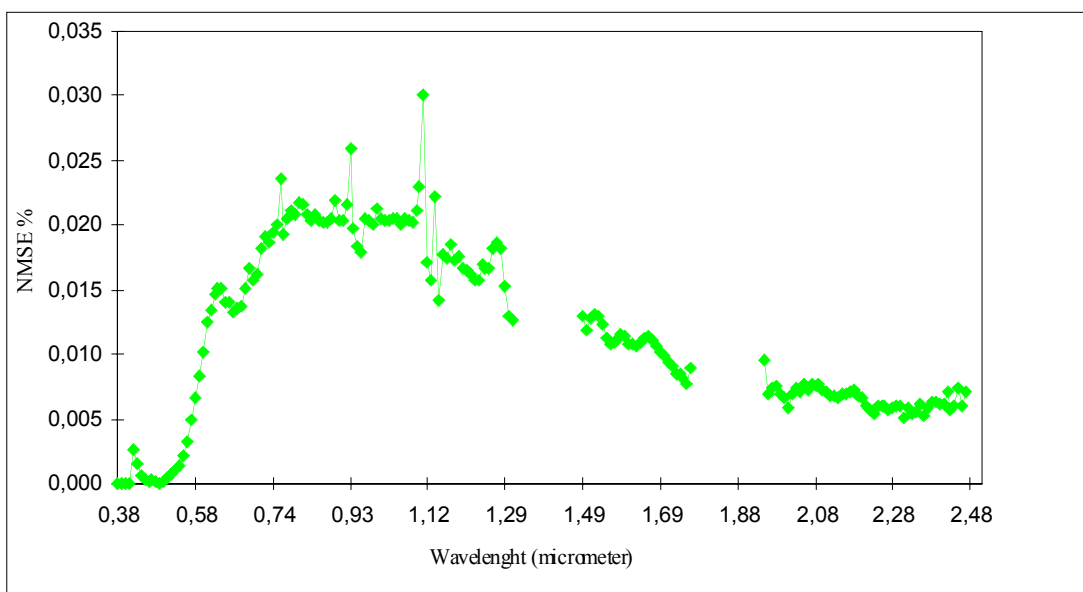Normalized mean square error between the two reflectance spectra (below)

Normalized Square Mean Error (%) on range (0,38-2,5μm)	12.68

Fig.5- Difference between the spectra corrected for atmospheric effects of a sample of body of water (08/25/1995 and 09/07/1995), in the spectral range from 0.38μm to 2.5μm, with its respective normalized mean square errors.
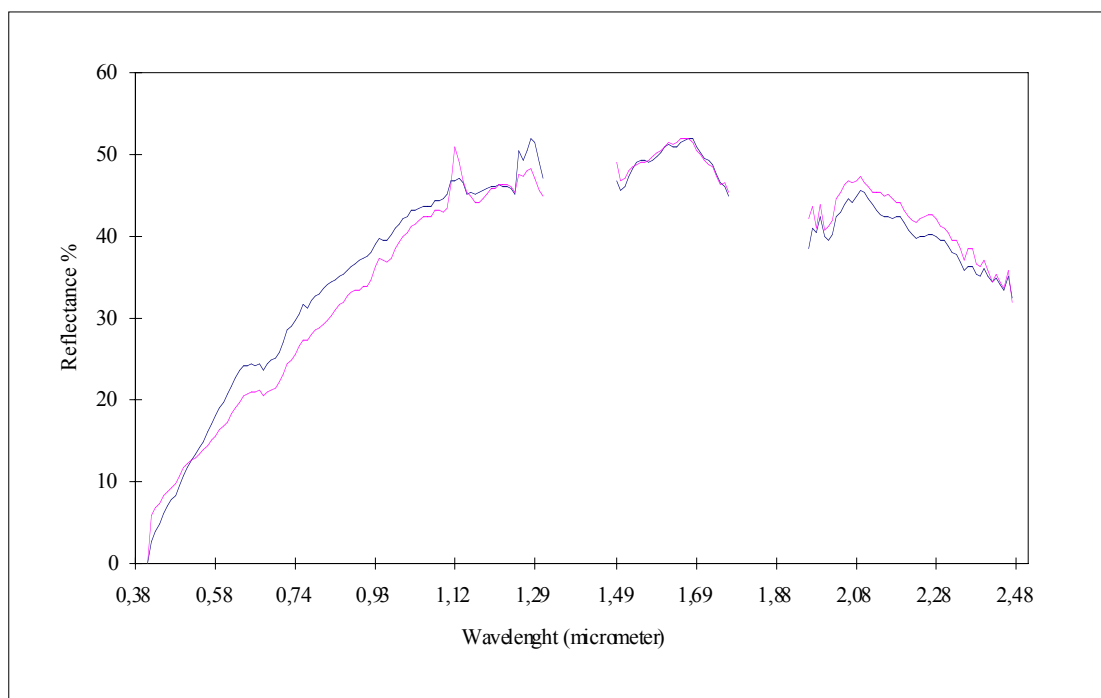
Normalized mean square error between the two reflectance spectra (below)

Normalized Square Mean Error (%) on range (0,38-2,5μm)	2.19

Fig.6 - Difference between the spectra corrected for atmospheric effects of a sample of bare soil (08/25/1995 and 08/27/1995), in the spectral range from 0.38μm to 2.5μm, with its respective normalized mean square errors.

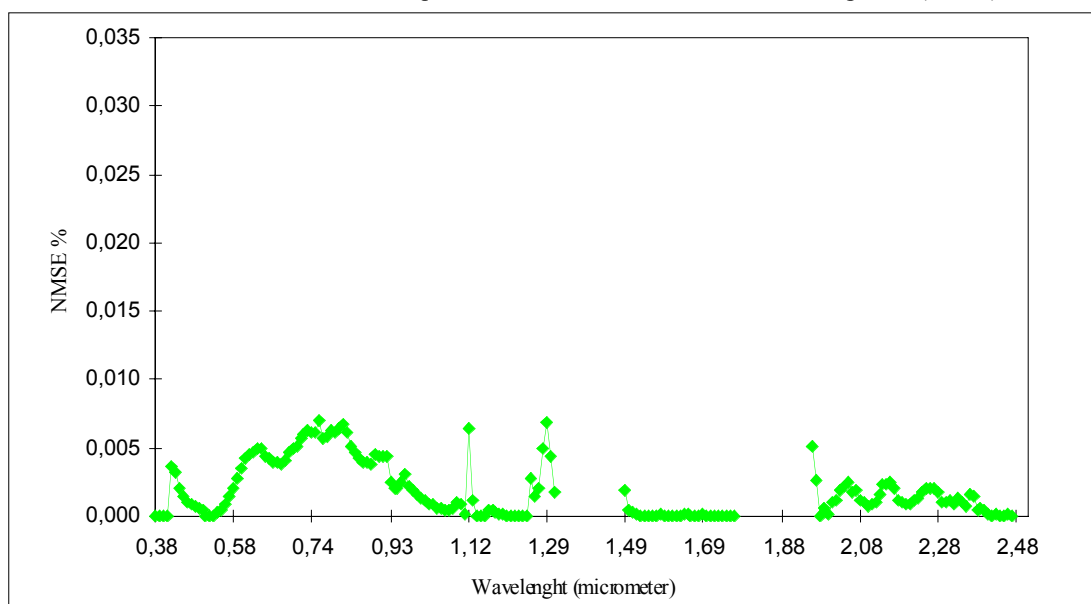Normalized mean square error between the two reflectance spectra (below)

Normalized Square Mean Error (%) on range (0,38-2,5μm)	0.35

Fig.7 - Difference between the spectra corrected for atmospheric effects of a sample of bare soil (08/25/1995 and 09/07/1995), in the spectral range from 0.38μm to 2.5μm, with its respective normalized mean square errors.

6. Conclusions

These results show that the illumination geometry introduces a strong influence in the results, so the minimization of these effects should always be attempted, when analyzing same targets corrected in different days and under different atmospheric conditions.

Bibliographical Reference

Bowker D. E.; Davis, R.E.; Myrick, D.L.; Stacy, k.; Jones, W. |T. **Spectral atmospheric correction in multitemporal studies**. International Journal of remote Sensing 10 (6): 1127-1134, 1989.

Crust, A.P. **Synthesis on the method of atmospheric correction of Green et al. (1993)**. São José of Campos, February 10, 1997. Personal communication.

Freire, M.L.F. **Correção atmosférica de imagens LANDSAT contaminadas pelo efeito de adjacência (Atmospheric Correction of LANDSAT Images Contaminated by the Adjacent Effect- Master Thesis in Meteorology)** - Federal University of Paraíba, Campina Grande, PB, Brazil, 1996.

Green, R.O.; Conel, J.E.; Roberts, D.A. **Estimation of aerosol optical depth, pressure elevation, water vapor and calculation of apparent surface reflectance from radiance measured by the Airborne Visible/Infrared Imaging Spectrometer (AVIRIS) using the radiative transfer code**. SPIE, VOL.1937, p.2-11, 1993.

Green, R.O. **Program of Simulation of the data AVIRIS for the Dados TM (LANDSAT)**. São José of Campos, November 17, 1997. Personal communication.

Latorre, M. L. **Utilização de um método de correção atmosférica para o processamento de dados hiperespectrais do sensos AVIRIS em Regiões tropicais (Use of a Method for Atmospheric Correction in Tropical Regions for AVIRIS Data** - MS Thesis, in Remote Sensing). National Institute for Space Research, INPE, São José dos Campos, SP, Brazil, 1998.

Pitas, I.; Venetsanopaulos, A.N. **Nonlinear digital filters: principles and applications**. Boston:Kluwer Academic Publishers, 1990, 392p.

Project RADAMBRASIL. Location of the area. in: Leaf SD-21 Cuiabá: Geology, Geomorphology, Pedologia, Vegetation, Potential Use of the Earth. Rio de Janeiro: MME/SG/Projeto RADAMBRASIL, p.29, 1982. (Rising of natural resources, 26)

Smoke, Clouds, and Radiation - Brazil (SCAR-B), Aug16 -Sept14, 1995. Hampton, VA: NASA. Langley Research Center, 1996. Field Mission Report.